



Random Perturbations of Heteroclinic Attractors

Author(s): Emily Stone and Philip Holmes

Source: *SIAM Journal on Applied Mathematics*, Vol. 50, No. 3 (Jun., 1990), pp. 726-743

Published by: [Society for Industrial and Applied Mathematics](#)

Stable URL: <http://www.jstor.org/stable/2101884>

Accessed: 22/04/2013 19:18

Your use of the JSTOR archive indicates your acceptance of the Terms & Conditions of Use, available at
<http://www.jstor.org/page/info/about/policies/terms.jsp>

JSTOR is a not-for-profit service that helps scholars, researchers, and students discover, use, and build upon a wide range of content in a trusted digital archive. We use information technology and tools to increase productivity and facilitate new forms of scholarship. For more information about JSTOR, please contact support@jstor.org.



Society for Industrial and Applied Mathematics is collaborating with JSTOR to digitize, preserve and extend access to *SIAM Journal on Applied Mathematics*.

<http://www.jstor.org>

RANDOM PERTURBATIONS OF HETEROCLINIC ATTRACTORS*

EMILY STONE† AND PHILIP HOLMES‡

Abstract. Estimates are derived for the mean recurrence time of orbits in the neighborhood of an attracting homoclinic orbit or heteroclinic cycle in an ordinary differential equation, subject to small additive random noise. The theory presented is illustrated with numerical simulations of several systems, including ones invariant under symmetry groups, for which such heteroclinic attractors are structurally stable. The physical implications of the work presented are briefly discussed.

Key words. heteroclinic and homoclinic orbits, symmetry, structurally stable heteroclinic cycles, random perturbation, intermittency, passage times

AMS(MOS) subject classifications. 34C28, 60H10, 34C35, 34F05

1. Introduction. It is well known that homoclinic and heteroclinic orbits, or saddle connections, are important in determining the global behavior of dynamical systems. Under appropriate conditions, transverse homoclinic orbits lead to chaotic motions via the presence of horseshoes (Smale [21], Silnikov [20], Guckenheimer and Holmes [11], Wiggins [22]). Homoclinic orbits are associated with the creation and annihilation of periodic orbits in “infinite period” bifurcations. However, homoclinic and heteroclinic cycles are structurally unstable in general ordinary differential equations for the following simple reason. A point q is called homoclinic to a fixed point p (respectively, heteroclinic to a pair of points p^+, p^-) if the orbit $\varphi_t(q)$ based at q approaches p as $t \rightarrow \pm\infty$ (respectively, approaches p^+ as $t \rightarrow +\infty$ and p^- as $t \rightarrow -\infty$). Thus, in the homoclinic case, q lies in the intersection of the stable and unstable manifolds $W^s(p)$, $W^u(p)$. Since locally the $\dim(W_{\text{loc}}^s) + \dim(W_{\text{loc}}^u) = n$ (the ambient phase space dimension) at q , two manifolds of dimension s and $u = n - s$ must intersect in n -space. Such an intersection cannot be transverse because the orbit through q is contained in both manifolds; hence it can be removed by an arbitrarily small perturbation (Chillingworth [9], Guckenheimer and Holmes [11]). Similar arguments apply to a heteroclinic cycle connecting a set of saddle points. Thus these “codimension one” phenomena typically occur only at isolated points in one-parameter families of vector fields.

The presence of symmetry groups under which the vector field is equivariant radically changes the picture. It has recently become clear that the requirement that a vector field and perturbations of it respect certain symmetries implies that heteroclinic cycles can occur in a structurally stable manner, although they do not *necessarily* occur (the phenomenon is not generic). One of the first physically significant examples occurred in Busse’s studies of convection patterns (Busse and Heikes [8], Busse [7]) in which a set of three ordinary differential equations, invariant under cyclic permutations of the variables, was shown to possess a heteroclinic cycle (cf. Guckenheimer and Holmes [12]). Busse also remarked on the importance of random perturbations in further “stabilizing” the behavior, as we will see. Subsequently, Aubry et al. [5] recognized the presence of heteroclinic cycles induced by $O(2)$ -symmetry in a model for boundary layer dynamics. This led to a study of the global behavior of an

* Received by the editors July 11, 1988; accepted for publication (in revised form) April 25, 1989. This research was partially supported by Office of Naval Research grant N 00014-85-K-0172.

† Department of Theoretical and Applied Mechanics, Cornell University, Ithaca, New York 14853. Present address, DAMTP, Silver Street, Cambridge CB3 9EW, United Kingdom.

‡ Department of Mathematics and Center for Applied Mathematics and the Department of Theoretical and Applied Mechanics, Cornell University, Ithaca, New York 14853.

$O(2)$ -equivalent normal form (Armbruster, Guckenheimer, and Holmes [2]) and its occurrence in the Kuramoto–Sivashinsky equation (Armbruster, Guckenheimer, and Holmes [3]). Simultaneously, independent studies of the same system and its appearance in Rayleigh–Bénard convection were carried out (Jones and Proctor [13], Proctor and Jones [17]). The existence of structurally stable heteroclinic cycles appears to be connected with physical phenomena such as intermittency and turbulent bursting (cf. Aubry et al. [5], Pomeau and Manneville [16]).

These symmetry induced cycles are not generally associated with chaotic behavior. Indeed, under suitable conditions on the eigenvalues of the saddle point, the cycles are asymptotically as well as structurally stable, and all orbits in their neighborhood approach them as $t \rightarrow +\infty$. Solutions spend increasing periods near the equilibria and the heteroclinic “events” become less frequent. As Busse realized, small random perturbations can significantly alter the behavior. While such perturbations may be too small to noticeably modify the vector field outside neighborhoods of the equilibria, the random and deterministic components are comparable near those points and the diffusive action of the former prevents typical solutions from lingering. Thus the global structure of the heteroclinic events is essentially unchanged, whereas the durations between successive events becomes random. However, a well-defined mean duration emerges.

In this paper we develop a simple theory to predict the probability distribution of times between events and its expectation as a function of the (largest) unstable eigenvalue at the saddle and the root mean square (r.m.s.) noise level in the limit that the latter is small. Other deterministic system parameters enter the theory at higher order. Following Silnikov [19], [20], we argue that the behavior of orbits near the heteroclinic cycle is dominated by that of the system linearized at the hyperbolic saddle points. We thus reduce our analysis to that of stable and unstable, linear, Ornstein–Uhlenbeck processes, for which complete solutions are available. As expected, our leading order term for the mean time coincides with the mean exit time estimates of Kifer [14] for random perturbations starting on the local stable manifold of a hyperbolic saddle point. This estimate can also be obtained from an intuitive argument involving random impulses (Farmer [10]). The analysis is contained in § 2. Section 3 contains simulations of simple linear and planar systems for which we illustrate and verify the theory. In § 4 more substantial simulations are described in which the four-dimensional $O(2)$ equivariant normal form of Armbruster, Guckenheimer, and Holmes [2] and the ten-dimensional boundary layer model of Aubry et al. [5] are studied. The paper concludes in § 5 with a discussion of the implications for models of physical processes. For background in deterministic dynamical systems, see Guckenheimer and Holmes [11]; for stochastic differential equations and random processes see Arnold [4] and Breiman [6].

Since our main concern is with random perturbations of symmetry induced cycles, we do not address the question of homoclinic bifurcations in this paper—either “generic” bifurcations in which homoclinic orbits are destroyed, as they are under variation of γ, β in the example of § 3, or of the $O(2)$ symmetric problems in which the heteroclinic cycle persists but loses stability. The behavior of such parametrized families would be an interesting subject for future study.

2. Mean passage time analysis. We consider a system of the form

$$(2.1) \quad \frac{dx}{dt} = f(x) + \varepsilon \xi(t), \quad x \in \mathbb{R}^n$$

under the following assumptions:

- (A1) For $\varepsilon = 0$, (2.1) has an asymptotically stable homoclinic orbit (respectively, heteroclinic cycle) to a hyperbolic saddle point p (respectively, a set of hyperbolic saddles p_1, p_2, \dots , having identical linearizations). Thus all solutions starting near the homoclinic orbit approach it as $t \rightarrow +\infty$.
- (A2) $\xi(t)$ is a vector-valued random process of zero mean whose components are independent and each of which is an independent identically distributed random variable.

We comment on (A1)–(A2). Hyperbolicity is equivalent to the linearization $Df(p)$ (respectively, $Df(p_i)$) having eigenvalues all with nonzero real part, which can be (partially) ordered, as follows:

$$(2.2) \quad \lambda_u \stackrel{\text{def}}{=} \text{Re}(\lambda_1) \geq \text{Re}(\lambda_2) \geq \dots \geq \text{Re}(\lambda_{k-1}) > 0 > \text{Re}(\lambda_k) \stackrel{\text{def}}{=} -\lambda_s \geq \dots \geq \text{Re}(\lambda_n).$$

Let $W^s(p)$, $W^u(p)$ denote the stable and unstable manifolds of p . Asymptotic stability of the homoclinic orbit is guaranteed by two properties: (1) that $W^u(p) \subset W^s(p)$, so that every orbit leading a δ_1 -neighborhood U_{δ_1} of p returns to a (possibly larger) neighborhood U_{δ_2} . This is stricter than simple existence of a homoclinic orbit: even in a planar system it requires a certain “topological” symmetry (cf. Fig. 1). (2) A linear condition that implies asymptotic stability (but which is not necessary) is that

$$(2.3) \quad \lambda_s > \lambda_u,$$

for the eigenvalues of (2.2). We will assume this stronger condition throughout. For completeness we sketch the analysis below. We sometimes call such an object a homoclinic attractor. The generalization to the heteroclinic situation is obvious.

To avoid dealing with correlated random excitations we make an additional simplifying assumption:

- (A3) The linearization $Df(p)$ (respectively, $Df(p_i)$) of (2.1) at the saddle point(s) is “block diagonal” in the sense that the stable and unstable eigenspaces are orthogonal at $p(p_i)$.

This assumption will imply that, when nonlinear terms are ignored, the stable and unstable subsystems evolve independently.

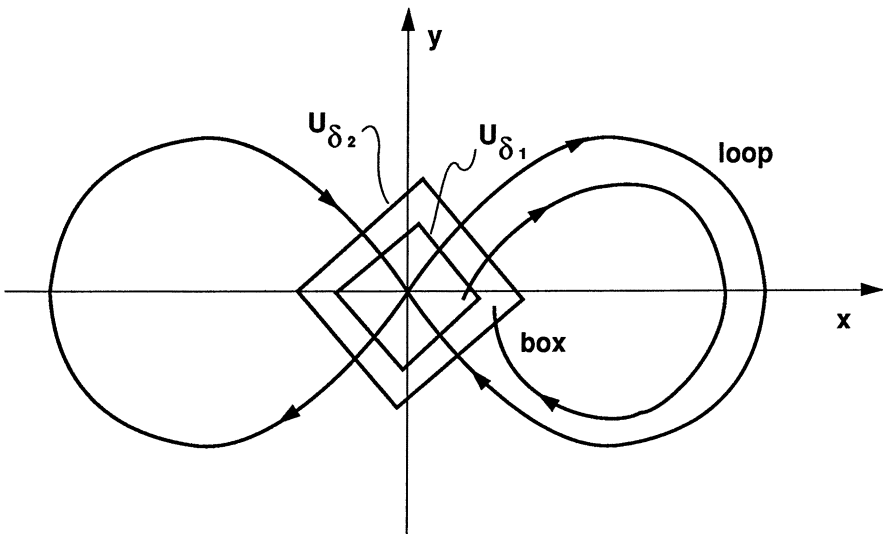


FIG. 1. A double homoclinic loop for the Duffing equation (cf. § 3.2).

The properties of $\xi(t)$ will be specified in more detail below. In practical applications $|\xi(t)|$ is usually bounded and thus as $\varepsilon \rightarrow 0$ we have a family of small random perturbations of a deterministic system with a homoclinic (or heteroclinic) attractor.

As we have noted, equivariance of the vector field $f(x)$ under a group Γ sometimes implies the existence of structurally stable heteroclinic cycles involving orbits $W^u(p_j) \cap W^s(p_{j+1})$ connecting a sequence p_1, p_2, \dots, p_s of saddle points, with $W^u(p_s) \subset W^s(p_1)$ closing the cycle (in Armbruster, Guckenheimer, and Holmes [2], [3], $s = 2$, in Busse [7] and Guckenheimer and Holmes [12], $s = 3$). However, equivariance implies that the saddles are all images of one another under a group element ($p_{j+1} = \gamma_j(p_1)$, $\gamma_j \in \Gamma$) and hence that the spectra of their linearizations are identical. The homoclinic analysis of § 2.1 extends to this situation with some significant changes: for example, we can still have attracting cycles even when (2.3) fails (cf. Armbruster, Guckenheimer, and Holmes [2] and see § 2.1 below). We can develop a more general theory for heteroclinic cycles connecting dissimilar saddles, but that is not necessary for our purposes.

With regard to (A2), strictly we should take $|\xi(t)|$ bounded, so that the random perturbation is uniformly small. However, to make explicit computations we will model $\xi(t)$ by a Wiener process, which can have unbounded excursions.

2.1. Stability of a deterministic homoclinic orbit. We first recall the analysis for $\varepsilon = 0$ (cf. Silnikov [19], [20], Guckenheimer and Holmes [11]). Choosing coordinates on the stable and unstable manifolds of p with origin at p , the linearized system decouples and the full system takes the form

$$(2.4) \quad \begin{aligned} \dot{x}_s &= [-A_s + f_s(x)]x_s, & x_s &\in W_{\text{loc}}^s(p), \\ \dot{x}_u &= [A_u + f_u(x)]x_u, & x_u &\in W_{\text{loc}}^u(p), \end{aligned}$$

where all eigenvalues of $-A_s$ (respectively, A_u) have negative (respectively, positive) real parts and f_s, f_u are $O(|x|)$. Let $\Pi_s = \{(x_u, x_s) \in U_\delta \mid |x_s| = \delta\}$ and $\Pi_u = \{(x_u, x_s) \in U_\delta \mid |x_u| = \delta\}$ be cross sections to the flow forming the $(n-1)$ -dimensional faces of a box of size 2δ centered at p (Fig. 2). Since $f_s, f_u = O(\delta)$ for $x = (x_s, x_u) \in U_\delta$, integration of (2.4) yields the estimates

$$(2.5a) \quad |x_s(t)| \leq |x_s(0)| e^{-(\lambda_s - c_1 \delta)t},$$

$$(2.5b) \quad |x_u(t)| \leq |x_u(0)| e^{(\lambda_u + c_1 \delta)t}$$

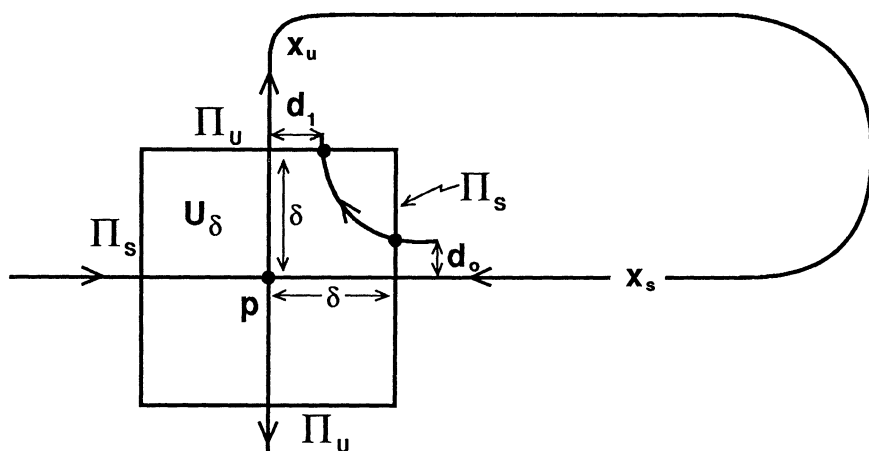


FIG. 2. Local stability analysis.

for some constant c_1 , where λ_s, λ_u are the constants defined in (2.2). From (2.5b) we estimate the minimum time of flight τ for solutions leaving Π_s to reach Π_u in terms of d_0 , the distance from the stable manifold on Π_s . We obtain

$$|e^{(\lambda_u + c_1 \delta)\tau}| \geq \frac{|x_u(\tau)|}{|x_u(0)|} = \frac{\delta}{d_0},$$

which yields

$$(2.6) \quad \tau \geq \frac{1}{\lambda_u + c_1 \delta} \ln \frac{\delta}{d_0}.$$

Equation (2.5a) sets an upper bound on the distance d_1 from the unstable manifold on exit:

$$\begin{aligned} |x_s(\tau)| &= d_1 \leq |x_s(0)| e^{-(\lambda_s - c_1 \delta)\tau} \\ &\leq \delta e^{(\lambda_s - c_1 \delta)/(\lambda_u + c_1 \delta)} \ln \left(\frac{\delta}{d_0} \right), \end{aligned}$$

or

$$(2.7) \quad d_1 \leq \delta^{1 - (\lambda_s - c_1 \delta)/(\lambda_u + c_1 \delta)} d_0^{(\lambda_s - c_1 \delta)/(\lambda_u + c_1 \delta)} \leq K_1 d_0^{\lambda_s/\lambda_u + O(\delta)}.$$

In the estimate above we use the fact that λ_s , the eigenvalue of A_s with smallest real part, provides a lower bound for the norm $|A_s|$ and hence that $e^{-\lambda_s \tau}$ provides an upper bound for the contractive properties of $e^{-A_s \tau}$. We conclude that, if (2.3) is satisfied and $\lambda_s/\lambda_u \geq \mu > 1$, we can pick δ small enough so that $(\lambda_s - c_1 \delta)/(\lambda_u + c_1 \delta) > 1$ and $d_0^{\lambda_s/\lambda_u + O(\delta)} = o(d_0)$.

Now consider the behavior of solutions leaving Π_u . Since there are no singular points in a sufficiently small tubular neighborhood of any homoclinic orbit to p outside of U_δ , the magnitude of the vector field is bounded below and consequently the time taken to return to U_δ on Π_s by solutions that do so is bounded above by, say, T , independent of d_0, d_1 (but depending on δ). Thus, simple estimates guarantee that the maximum distance from $W_s(p)$ on reentry to U_δ is bounded above by $e^{c_2 T} d_1 \stackrel{\text{def}}{=} c_3 d_1$. Thus, using (2.7) and taking $0 < d_0 < \delta \ll 1$ sufficiently small, we have

$$(2.8) \quad c_3 d_1 \leq c_3 K_1 d_0^{\lambda_s/\lambda_u + O(\delta)} < d_0.$$

This implies that the homoclinic orbit attracts all solutions that reenter U_δ . But the global topological assumption that $W^u(p) \subset W^s(p)$ guarantees that all solutions leaving Π_u must reenter U_δ .

In the case of equivariant vector fields certain directions are “irrelevant” and this leads to improved estimates at (2.6)–(2.7). In particular, as shown in Armbruster, Guckenheimer, and Holmes [2], $O(2)$ -equivariant vector fields always have a zero eigenvalue with eigenvector tangent to orbits of the group action. (The spectrum of eigenvalues is $-\lambda_{s_1} < -\lambda_{s_2} < 0 < \lambda_u$.) However, since there is no component of $f(x)$ in this direction, we can ignore the zero eigenvalue. Moreover, a weakly stable eigenvalue λ_{s_2} can also be ignored, since its eigenvector lies in an invariant plane and the global structure of the vector field implies that a solution that diverges from the saddle p_1 is strongly attracted when it passes p_2 , so that the net effect of a passage by both saddles in the cycle is attractive provided that $\lambda_u < \lambda_{s_1}$, even though $\lambda_{s_2} < \lambda_u$.

2.2. A model for random perturbations. We split our analysis into local and global regions much as above. Since $|f(x)| > K\delta$ outside U_δ , and we are concerned with the

limit of small noise ($0 < \varepsilon \ll \delta$), we will assume that the solution outside U_δ is essentially unaffected. In particular, we still have estimates on the return time to Π_s for orbits leaving U_δ via Π_u :

$$(2.9) \quad K_2 + c_4 \varepsilon \leq T \leq K_3 + c_5 \varepsilon,$$

where K_2, K_3 depend only on δ . The bounds in (2.9) come from integration of the expression $\tilde{K}_2 - \tilde{c}_4 \varepsilon \leq |\dot{x}| \leq \tilde{K}_3 + \tilde{c}_5 \varepsilon$, which applies to (2.1) outside a neighborhood of fixed points, together with the fact that solutions leaving U_δ near the homoclinic orbit travel a finite distance before entering U_δ again. Thus the leading effect of noise is felt in U_δ , where $\varepsilon|\xi(t)|$ and $|f(x)|$ are comparable. To investigate this we model the dynamics in U_δ as a linear stochastic differential equation: an Ornstein-Uhlenbeck process.

As shown in (2.1) the growth of solutions in U_δ is dominated by the component in the strong unstable manifold, tangent to the eigenvectors of λ_u , whereas the contractive properties are dominated by the weakest stable eigenvalue $-\lambda_s$. Thus it is appropriate to take the simple model:

$$(2.10a) \quad dx = -\lambda_s x dt + \varepsilon dW_x,$$

$$(2.10b) \quad dy = \lambda_u y dt + \varepsilon dW_y,$$

where we take dW_x and dW_y to be zero mean, independent Wiener processes, i.e., $\langle dW_{x,y} \rangle = 0$, $\langle dW_{x,y}^2 \rangle = dt$, where $\langle \cdots \rangle$ denotes expectation. Thus ε is the r.m.s. noise level.

While the linearization of (2.1) with $\varepsilon = 0$ can always be diagonalized and hence decoupled, whether (A3) holds or not, the transformation affecting this will generally couple the components of the random process $\xi(t)$. However, if (A3) holds, and so only a *rotation* is necessary, the diffusion matrix in the Kolmogorov equation (2.11) below is still diagonal. Orthogonality holds approximately in the Duffing example of § 3 and exactly in the main, $O(2)$ symmetric example of § 4. Failure of (A3) would require the analysis of the vectorial analogue of (2.11) with a nondiagonal diffusion matrix.

If $p_t(x|x_0)$, $p_t(y|y_0)$ denote the conditional probability density functions for solutions of (2.10) started at x_0, y_0 at $t = 0$, then p_t obeys the forward Kolmogorov (or Fokker-Planck) equation

$$(2.11) \quad \frac{\partial}{\partial t} p_t = -\lambda \frac{\partial}{\partial z} (z p_t) + \frac{\varepsilon^2}{2} \frac{\partial^2}{\partial z^2} p_t,$$

with $\lambda = -\lambda_s, \lambda_u$ and $z = x, y$, respectively. The solution for the stable (x) process is well known (cf. Breiman [6]) and that for the unstable (y) process is analogous. If

$$(2.12) \quad \mathcal{N}(\mu, \sigma^2) = \frac{1}{\sqrt{2\pi\sigma^2}} e^{-(z-\mu)^2/2\sigma^2}$$

denotes the normal (Gaussian) distribution with mean μ and variance σ , then it is easy to check that

$$(2.13a) \quad p_t(x|x_0) = \mathcal{N}\left(x_0 e^{-\lambda_s t}, \frac{\varepsilon^2}{2\lambda_s} (1 - e^{-2\lambda_s t})\right),$$

and

$$(2.13b) \quad p_t(y|y_0) = \mathcal{N}\left(y_0 e^{\lambda_u t}, \frac{\varepsilon^2}{2\lambda_u} (e^{2\lambda_u t} - 1)\right)$$

solve (2.11) with $p_0(x|x_0) = \mathcal{N}(x_0, 0)$, $p_0(y|y_0) = \mathcal{N}(y_0, 0)$. It is also useful to observe that, if the unstable process is started with a normal distribution $\mathcal{N}(y_0, \sigma_{y_0}^2)$ rather than at the point $y = y_0$, $(\mathcal{N}(y_0, 0))$, we have

$$(2.14) \quad p_t(y|\mathcal{N}(y_0, \sigma_{y_0}^2)) = \mathcal{N}\left(y_0 e^{\lambda_u t}, \sigma_{y_0}^2 e^{2\lambda_u t} + \frac{\varepsilon^2}{2\lambda_u} (e^{2\lambda_u t} - 1)\right)$$

and that (2.14) is equivalent to the distribution achieved by the same process started with a δ -function $\mathcal{N}(y'_0, 0)$ at the earlier time $t = -t'$, where

$$(2.15) \quad t' = \frac{1}{2\lambda_u} \ln\left(\frac{2\sigma_{y_0}^2 \lambda_u}{\varepsilon^2} + 1\right), \quad y'_0 = y_0 \left(\frac{2\sigma_{y_0}^2 \lambda_u}{\varepsilon^2} + 1\right)^{-1/2}.$$

A similar expression holds for $p_t(x|\mathcal{N}(x_0, \sigma_{x_0}^2))$.

Since the means $\mu_x = \langle x \rangle$, $\mu_y = \langle y \rangle$ evolve according to the deterministic equations

$$(2.16) \quad \frac{d}{dt} \mu_x = -\lambda_s \mu_x, \quad \frac{d}{dt} \mu_y = \lambda_u \mu_y,$$

we conclude from the analysis of § 2.1 that on exit from U_δ via Π_u , we have

$$(2.17) \quad \mu_x \leq c_3 K_1 \mu_y^{\lambda_s/\lambda_u + O(\delta)}$$

(cf. (2.7)). Thus, using the estimate (2.9) we can conclude that, for $\mu_x(t)$ sufficiently small at time $t = 0$, $\mu_y(t) \rightarrow 0$ as $t \rightarrow +\infty$: randomly perturbed solutions still converge to the homoclinic attractor in mean. Here μ_x and μ_y play the roles of d_1 and d_0 . Thus the long-term incoming solutions on Π_s are centered at $y = 0$. Furthermore, since the time of flight through U_δ for unperturbed solutions goes to ∞ as $d_0(\mu_y) \rightarrow 0$ (2.6), we can expect the distribution $p_t(x|\mathcal{N}(x_0, \sigma_{x_0}^2))$ to approach its asymptotic value for $t \rightarrow \infty$ (cf. (2.13a))

$$(2.18) \quad p_t(x|\mathcal{N}(x_0, \sigma_{x_0}^2)) = \mathcal{N}\left(0, \frac{\varepsilon^2}{2\lambda_s}\right).$$

Finally, since the outgoing x -distribution is, to first order, the incoming y distribution (cf. Figs. 1 and 2), we obtain from (2.14) that

$$(2.19) \quad p_t\left(y|\mathcal{N}\left(0, \frac{\varepsilon^2}{2\lambda_s}\right)\right) = \mathcal{N}\left(0, \frac{\varepsilon^2}{2\lambda_s} e^{2\lambda_u t} + \frac{\varepsilon^2}{2\lambda_u} (e^{2\lambda_u t} - 1)\right).$$

We now use the expression (2.19) to estimate the mean time required to pass through U_δ from Π_s to Π_u . We note that Kifer [14] has solved a more general, multidimensional nonlinear problem in the limit $\varepsilon \rightarrow 0$ for the expected exit time for solutions starting on $W^s(p) \cap \{p\}$. Here, however, we have an initial distribution centered on $W^s(p)$ with variance $\varepsilon^2/2\lambda_s$. We will compare our result with his below. We first observe that, from (2.14)–(2.15), in place of (2.19), it suffices to consider a process

$$(2.20) \quad p_s(y|0) = \mathcal{N}\left(0, \frac{\varepsilon^2}{2\lambda_u} (e^{2\lambda_u s} - 1)\right)$$

started at time $s = 0$ with $s = t + t'$ and

$$(2.21) \quad t' = \frac{1}{2\lambda_u} \ln\left(1 + \frac{\lambda_u}{\lambda_s}\right).$$

The probability that the passage time T exceeds t is therefore the probability that a solution started at $y=0$, $(\mathcal{N}(0, 0))$, is still in U_δ at time $s=t+t'$, or

$$(2.22) \quad P(T > s) = \int_{-\delta}^{\delta} p_s(y|0) dy.$$

It follows that the mean passage time $\tau = \langle T \rangle$ is given by

$$(2.23) \quad \tau = \int_0^\infty P(T > t) dt = \int_{t'}^\infty P(T > s) ds.$$

To compute $P(T > s)$, we use (2.22), (2.20), and (2.12) and define

$$(2.24) \quad Y = y \left(\frac{\varepsilon^2}{\lambda_u} (e^{2\lambda_u s} - 1) \right)^{-1/2},$$

$$\Delta = \Delta(s) = \delta \left(\frac{\varepsilon^2}{\lambda_u} (e^{2\lambda_u s} - 1) \right)^{-1/2},$$

so that the integral of (2.22) yields

$$(2.25) \quad P(T > s) = 2 \int_0^{\Delta(s)} \frac{1}{\sqrt{\pi}} e^{-Y^2} dY = \operatorname{erf}(\Delta(s)).$$

We therefore have

$$(2.26) \quad \tau = \int_{t'}^\infty \operatorname{erf}(\Delta(s)) ds = \frac{1}{\lambda_u} \int_{\lambda_u t'}^\infty \operatorname{erf} \left(\frac{\delta}{\varepsilon} \left(\frac{\lambda_u}{e^{2\sigma} - 1} \right)^{1/2} \right) d\sigma.$$

Equation (2.26) may be reexpressed in a form more convenient for computation. Letting $\eta^2 = \delta^2 \lambda_u / \varepsilon^2 (e^{2\sigma} - 1)$ and recalling (2.21), we obtain

$$(2.27) \quad \tau = \frac{1}{\lambda_u} \int_0^{\delta \sqrt{\lambda_s} / \varepsilon} \operatorname{erf}(\eta) \frac{d\eta}{\eta (1 + \varepsilon^2 \eta^2 / \delta^2 \lambda_u)}.$$

Integrating by parts and evaluating the boundary term, we obtain

$$(2.28) \quad \tau = -\frac{1}{2\lambda_u} \left\{ \operatorname{erf} \left(\frac{\delta}{\varepsilon} \sqrt{\lambda_s} \right) \ln \left(1 + \frac{\lambda_u}{\lambda_s} \right) - \int_0^{\delta \sqrt{\lambda_s} / \varepsilon} \ln \left(1 + \frac{\delta^2 \lambda_u}{\varepsilon^2 \eta^2} \right) \frac{2}{\sqrt{\pi}} e^{-\eta^2} d\eta \right\}.$$

Since $\operatorname{erf}(x) \rightarrow 1$ as $x \rightarrow \infty$ and $\lambda_u < \lambda_s$, the leading term in the braces is uniformly bounded for all ε . In fact it vanishes in the limit $\lambda_u / \lambda_s \rightarrow 0$ (a strongly stable homoclinic orbit). The dominant behavior in ε therefore comes from the integral, the integrand of which may be expanded in a Taylor series:

$$\ln \left(1 + \frac{\delta^2 \lambda_u}{\varepsilon^2 \eta^2} \right) = \ln \left(\frac{\delta^2 \lambda_u}{\varepsilon^2 \eta^2} \left(1 + \frac{\varepsilon^2 \eta^2}{\delta^2 \lambda_u} \right) \right) = \ln \left(\frac{\delta^2 \lambda_u}{\varepsilon^2 \eta^2} \right) + \frac{\varepsilon^2 \eta^2}{\delta^2 \lambda_u} + O(\varepsilon^4 \eta^4),$$

so that (2.28) may be written

$$\tau = -\frac{1}{2\lambda_u} \left\{ \operatorname{erf} \left(\frac{\delta}{\varepsilon} \sqrt{\lambda_s} \right) \ln \left(1 + \frac{\lambda_u}{\lambda_s} \right) - \int_0^{\delta \sqrt{\lambda_s} / \varepsilon} \ln \left(\frac{\delta^2}{\varepsilon^2} \right) \frac{2}{\sqrt{\pi}} e^{-\eta^2} d\eta \right. \\ \left. - \int_0^{\delta \sqrt{\lambda_s} / \varepsilon} \ln \left(\frac{\lambda_u}{\eta^2} \right) \frac{2}{\sqrt{\pi}} e^{-\eta^2} d\eta + O(\varepsilon^2) \right\},$$

or

$$(2.29) \quad \tau = \frac{1}{\lambda_u} \left\{ \ln \left(\frac{\delta}{\varepsilon} \right) \operatorname{erf} \left(\frac{\delta}{\varepsilon} \sqrt{\lambda_s} \right) + O(1) + O(\varepsilon^2) \right\},$$

where the $O(1)$ and $O(\varepsilon^2)$ terms can be calculated explicitly from (2.28). Finally, in the limit $\varepsilon \rightarrow 0$, since $\varepsilon \ll \delta$, we can use the estimate of $\operatorname{erf}((\delta/\varepsilon)\lambda_s) = 1 + O(\varepsilon)$ to write

$$(2.30) \quad \tau \sim \frac{1}{\lambda_u} \left\{ \ln \left(\frac{\delta}{\varepsilon} \right) + O(1) \right\}.$$

As expected, this agrees with Kifer's result that

$$\lim_{\varepsilon \rightarrow 0} P \left\{ 1 - \gamma < \frac{\tau \lambda_u}{|\ln(\varepsilon)|} < 1 + \gamma \right\} = 1$$

for any $\gamma > 0$ (Kifer [14, Thm. 2.1]); however, our simpler linear model has permitted us to compute the expression (2.27) valid for an arbitrary ε and to include the effect of an initial distribution. Indeed the expression (2.25) permits us to compute the complete probability distribution in closed form. Let $P(s)$ denote the probability distribution function for passage times (in terms of $s = t + t'$); we then have

$$(2.31) \quad \begin{aligned} P(s) &= \frac{d}{ds} (1 - P(T > s)) = -\frac{d}{ds} \operatorname{erf}(\Delta(s)) \\ &= -\frac{2}{\sqrt{\pi}} e^{-\Delta^2(s)} \Delta'(s) \\ &= \frac{2\lambda_u \Delta(s) e^{-\Delta^2(s)}}{\sqrt{\pi}(1 - e^{-2\lambda_u s})}, \end{aligned}$$

with $\Delta(s)$ given by (2.24). The analogous expression in terms of t is easily obtained using $s = t + t'$ and (2.21). Returning to the global homoclinic problem, we recall from (2.9) that the return time for solutions outside U_δ is uniformly bounded, and so can be combined with the $O(1)$ constant in (2.30) to yield our final estimate for mean passage time:

$$(2.32) \quad \tau_p = K_0 + \frac{1}{\lambda_u} (|\ln(\varepsilon)| + K_1),$$

where the K_i are constants independent of ε but depending on δ , λ_s , λ_u and the vector field $f(x)$ near the homoclinic loop outside U_δ . However, the dependence on δ is not really relevant; it just corresponds to selection of a "local" neighborhood, which we can do once and for all. Also see § 3. In the absence of detailed a priori estimates of the global return time T (eq. (2.9)), this seems to be the most convenient form of passage time prediction to use. The constants K_i are to be fitted to the data and we envisage using (2.32) to test for the presence of homoclinic cycles in noisy numerical simulations or experimental data.

We end this section by noting that the extremely simple discrete model, in which a single random impulse of average size ε is applied at each pass through U_δ , proposed by Farmer [10], yields the same result. Durrett remarks that this is due to the fact that once the solution has left the ε -neighborhood of the stable manifold, the deterministic vector field dominates so that the remaining part of the exit time is $O(1)$ (also cf. Kifer [14, Thm. 2.3]). We also remark that the expression (2.27) can be obtained by seeking the centroid of the distribution

$$(2.33) \quad \int_{-\infty}^{-\delta} p_s(y, 0) dy + \int_{\delta}^{\infty} p_s(y, 0) dy$$

of solutions that have exited U_δ at time s .

3. Verification of the local model: simulations of a linear system and Duffing's equation. To test the assumptions about the equilibration of exit distributions $p_t(y) \rightarrow p_\infty(x) = \mathcal{N}(0, \varepsilon^2/2\lambda_s)$ (eq. (2.18)) and to see how well the $\varepsilon \rightarrow 0$ limit of (2.30) behaves, we performed numerical simulations of the two independent stochastic differential equations (2.10a), (2.10b). We also checked the probability density function of (2.31) against simulations. In all the numerical experiments described below we simulated the Wiener processes with the random number generator of the SUN C-library. This routine, `random()`, returns pseudorandom numbers in the range $(0 \rightarrow (2^{31} - 1))$ with a period of $\sim 16(2^{31} - 1)$. Thus the amplitude distribution is of boxcar type rather than flat to infinity. We normalized the numbers to zero mean and unit variance. Computations were performed in double precision C using fourth-order Runge-Kutta integrations with stepsize 0.05.

Figure 3 shows the results of simulations for the case $\lambda_s = 1.0$ with varying r.m.s. noise ε (Fig. 3(a)) and varying unstable eigenvalue λ_u (Fig. 3(b)). In all cases the size δ of the neighborhood was fixed at $\delta = 1$ and an ensemble average of solutions with initial conditions $(x_0, y_0) = (1, 0)$ was taken. In this way we are able to test the accuracy of our theory in the case where the initial distribution is a delta function $p_0 = \mathcal{N}(0, 0)$ (eq. (2.18)). Thus in Figs. 3(a) and 3(b) we show simulations compared with the exact expression of (2.27)–(2.28) with the upper limit of integration replaced by ∞ , and in Fig. 3(c) with the probability distribution of passage times of (2.31), noting that here $s = t$ since $t' = 0$ for solutions starting at $y_0 = 0$ with zero variance. In Fig. 3(a) we also show the leading term (2.30) of the mean time expression to illustrate that it does capture the correct asymptotic behavior as $\varepsilon \rightarrow 0$.

To check the validity of our assumption of long-term equilibration to an exit distribution $p_\infty = \mathcal{N}(0, \varepsilon^2/2\lambda_s)$ (eq. (2.18)) we next integrated the same linear process but reinjected the solutions exiting U_δ on $|y| = \delta$, $|x| = x_{\text{exit}}$ at points $|x| = \delta$; $y = x_{\text{exit}}$. After repeated passes through U_δ the process did indeed equilibrate and Fig. 3(d) shows the measured exit distribution compared with equation (2.18). However, the distributions take a long time to converge, for even after 1,000 trips around the cycle there is a significant central deviation, although the ratio of the eigenvalues λ_s/λ_u is two and the cycle is fairly strongly attracting. Finally, Fig. 3(e) shows mean passage times versus ε for the reinjected process for two values of λ_u and again the comparison with the theory of (2.27)–(2.28) is excellent. We also show the theory evaluated with upper limit set to ∞ , corresponding to neglect of the input variance ($p_\infty = \mathcal{N}(0, 0)$) and note that the small initial variance of $\varepsilon^2/2\lambda_s$ has only a minor effect on the predictions. In any case, it does not explicitly enter the asymptotic expression (2.30), since it only contributes a piece of $O(\varepsilon \ln(1/\varepsilon))$ to the $O(1)$ error term.

To test the validity of our assumptions of bounded perturbations on the “global” leg of passage around a homoclinic cycle (eq. (2.9)) we next integrated the Duffing equation

$$(3.1) \quad \begin{aligned} dx &= y \, dt + \varepsilon \, dW_x, \\ dy &= (x - x^3 - \gamma y + \beta x^2 y) \, dt + \varepsilon \, dW_y. \end{aligned}$$

For small β, γ , the deterministic part of (3.1) may be diagonalized at $(0, 0)$ by a rotation, so that, in the analogue of (2.10), dW_x and dW_y are replaced by $(dW_x - dW_y)/\sqrt{2}$ and $(dW_x + dW_y)/\sqrt{2}$, respectively. Each process is still perturbed by a Wiener process of zero mean and expectation:

$$\frac{1}{2}(\langle (dW_x \pm dW_y)^2 \rangle) = \frac{1}{2}(\langle dW_x^2 \rangle + \langle dW_y^2 \rangle) = dt$$

and the analysis of § 2 applies. For larger γ a correction to the expectation is necessary.

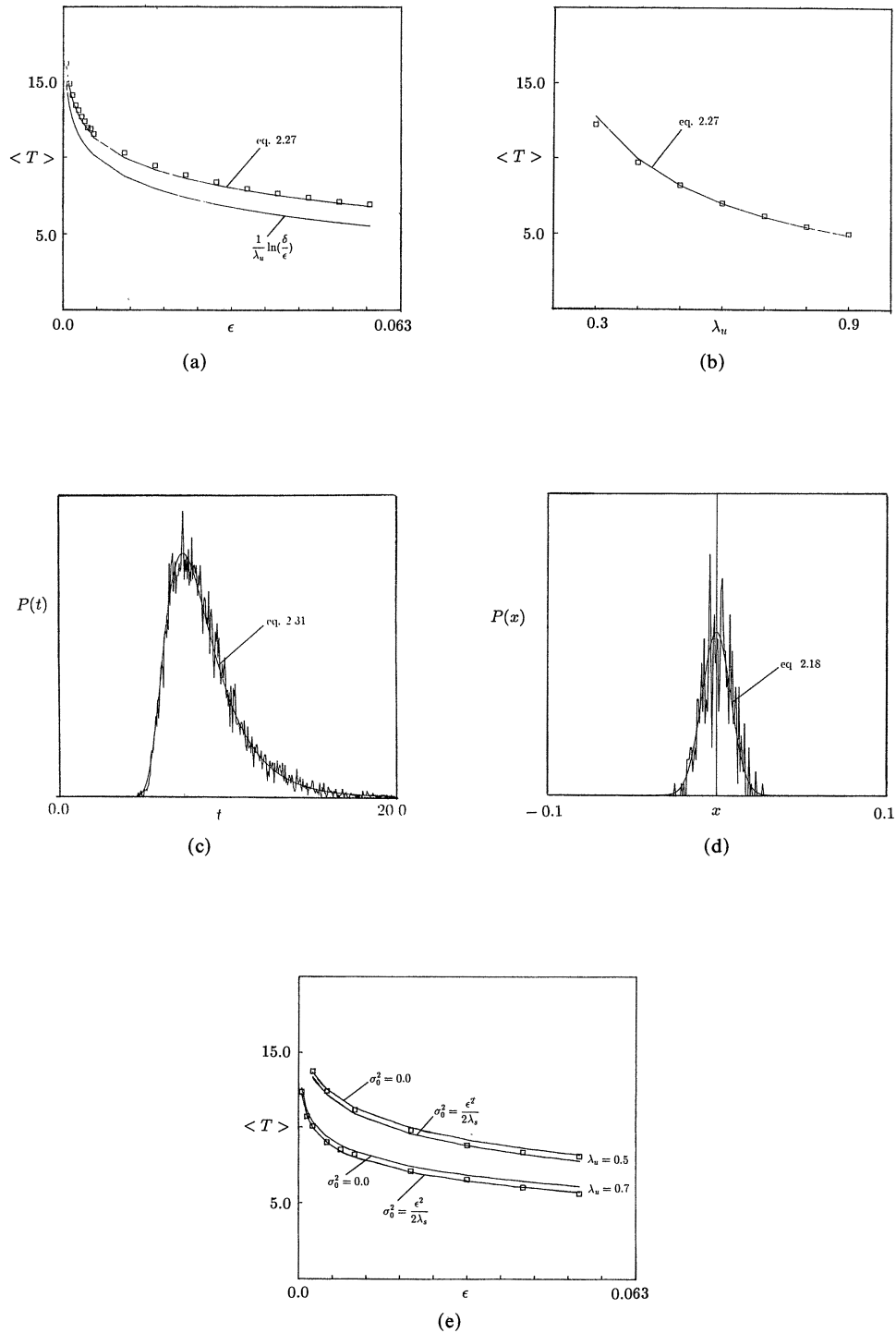


FIG. 3. Simulations of the linear process (2.10a), (2.10b), $\lambda_s = 1.0$, $\delta = 1.0$. Simulation results shown as square boxes. (a) Mean passage time for $\lambda_u = 0.5$, various ϵ , 1,000 trials. (b) Mean passage time for $\epsilon = 0.03$, various λ_u , 1,000 trials. (c) Passage time distribution for $\lambda_u = 0.5$, $\epsilon = 0.03$, 10,000 trials. (d) Exit distribution for $\lambda_u = 0.5$, $\lambda_s = 1.0$, $\epsilon = 0.03$, 261 trials. (e) Mean passage times for $\lambda_u = 0.5, 0.7$, various ϵ , 100 reinjections each.

For $\varepsilon = 0$, it is known that there exists a curve $\beta = \beta(\delta)$ on which (3.1) has a double attracting homoclinic cycle (cf. Fig. 1). In fact, it is easy to compute that $\beta = 5\gamma/4 + O(\gamma^2)$ by the “Melnikov” perturbation method (cf. Guckenheimer and Holmes [11]). Careful selection of β , γ near the line $\beta = 5\gamma/4$ by numerical search therefore yields a nonlinear system possessing a pair of attracting homoclinic cycles. Here we took $\delta = 0.1$ and aligned the box U_δ with edges parallel to the stable and unstable eigenvalues at the origin. We considered two cases, $\beta = 0.498$, $\gamma = 0.4$, which yield $\lambda_s = 1.22$, $\lambda_u = 0.82$, and $\beta = 0.1$, $\gamma = 0.08$, and $\lambda_s = 1.04$, $\lambda_u = 0.96$. The eigenvalues are computed via the formula $\lambda_{u,s} = \frac{1}{2}(-\gamma \pm \sqrt{\gamma^2 + 4})$ obtained by linearizing the equation at the saddle point.

We show the mean passage times through U_δ and around the entire loop separately for the two cases in Fig. 4(a) and 4(b). Here the “global” loop time T can easily be estimated for a specific choice of δ from the time taken by solutions in the unperturbed homoclinic loop to pass from the exit point(s) $(x, y) = (\pm\delta/\sqrt{2}, \pm\delta/\sqrt{2})$ to the entry point(s) $(\pm\delta/\sqrt{2}, \mp\delta/\sqrt{2})$. Since the unperturbed homoclinic solution is given by $x(t) = \sqrt{2} \operatorname{sech}(t)$, this time is obtained by solving

$$\frac{\delta}{\sqrt{2}} = \sqrt{2} \operatorname{sech}\left(\frac{T}{2}\right) \Rightarrow T = 2 \operatorname{sech}^{-1}\left(\frac{\delta}{2}\right),$$

or

$$(3.2) \quad T \approx 7.377$$

for $\delta = 0.1$. Figures 4(a) and 4(b) show the mean passage times τ for U_δ and $\tau + T$. Agreement with our simple theory is again excellent, in particular the estimate of (3.2) for the global loop time is accurate and the simulations show no significant effect of noise on this component of the passage times. Finally, Figs. 4(c) and 4(d) show probability density functions of solutions exiting the neighborhood U_δ on Π_u and entering it on Π_s , compared with our equilibrium prediction of (2.18). We see that the simulations agree reasonably well with the predicted zero mean Gaussian distribution. The central deviation in the distribution is again the result of a limited sample run and slow convergence to the normal distribution. Figure 4(e) illustrates that the linear dependence of the variance on mean square noise level ε^2 is valid.

4. Random perturbation of heteroclinic cycles in $O(2)$ symmetric systems. As described in the Introduction, while homoclinic and heteroclinic cycles are usually structurally unstable phenomenon, and hence the effects of noise on them may not appear to be of interest in a general context, in systems with symmetry such cycles can occur stably. In particular, heteroclinic cycles connecting hyperbolic saddle points occur for open sets of parameters in the unfolding of $O(2)$ equivalent normal forms near certain degenerate bifurcation points. Such systems describe the interaction of two complex Fourier coefficients of wave numbers $k, 2k$ in partial differential equations, which are invariant under spatial translation and reflection (cf. Armbruster, Guckenheimer, and Holmes [2], [3], Proctor and Jones [17]). Since this symmetry is common in physical systems and their idealizations, we feel that it is especially useful to study the effects of noise in this case. We note that the additive random perturbations do not respect the $O(2)$ equivariance, but that the perturbed systems remain close to systems with heteroclinic cycles.

In this section we report simulations of the system

$$(4.1) \quad \begin{aligned} \dot{z}_1 &= \bar{z}_1 z_2 + (\mu_1 + e_{11}|z_1|^2 + e_{12}|z_2|^2)z_1 + \varepsilon \xi_1(t), \\ \dot{z}_2 &= -z_1^2 + (\mu_2 + e_{21}|z_1|^2 + e_{22}|z_2|^2)z_2 + \varepsilon \xi_2(t), \end{aligned}$$

where $(z_1, z_2) \in C^2$, ξ_1, ξ_2 are complex-valued independent random processes with

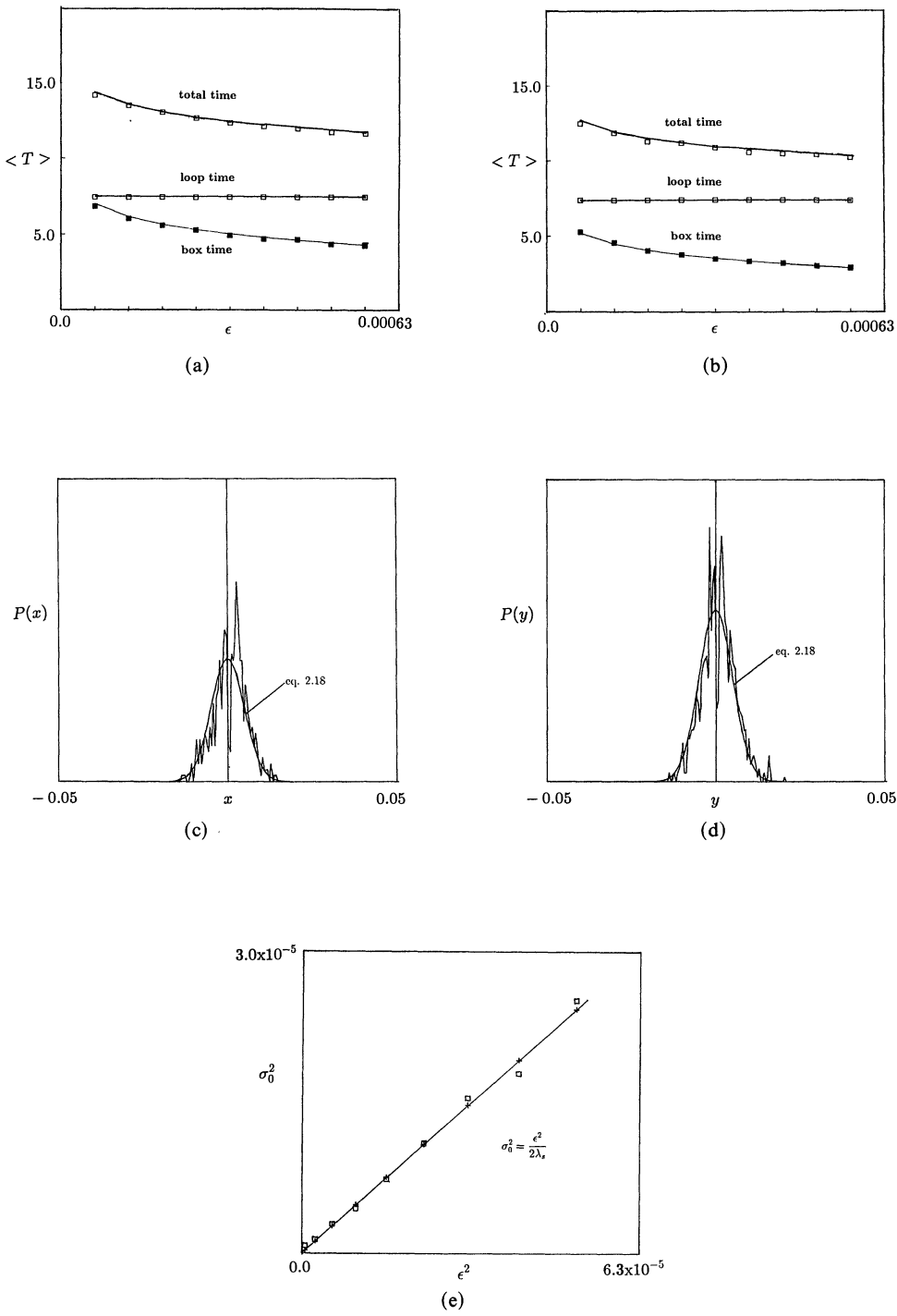


FIG. 4. Simulations of the Duffing equation (3.1), sample size = 1,000 trials in each case. (a) $\gamma = 0.4$, $\beta = 0.498$, various ϵ . (b) $\gamma = 0.08$, $\beta = 0.1$, various ϵ . Plots show mean passage time through B_δ , $\delta = 0.1$ and around homoclinic loop(s) compared with (2.27)–(2.28) and (2.27)–(2.28) plus global loop time. (c) Exit distribution for $\gamma = 0.4$, $\beta = 0.498$, $\epsilon = 0.0006$. (d) Incoming distribution for $\gamma = 0.4$, $\beta = 0.498$, $\epsilon = 0.0006$. (e) Variance of exit distribution versus mean square noise level ϵ^2 .

independent real and imaginary components and μ_j , e_{ij} are real parameters, chosen in the range in which (4.1) with $\varepsilon = 0$ has a set of attracting heteroclinic cycles. Linearizing at the saddles reveals that (4.1) is already in diagonal form. Reference [2] contains a complete analysis of the problem for $\varepsilon = 0$, and we have taken $e_{11} = -4.0$, $e_{12} = -1.0$, $e_{21} = e_{22} = -2.0$ (cf. Figs. 3 and 4 of [2]). For related work on a system possessing a heteroclinic cycle as a result of a discrete symmetry group, see Busse and Heikes [8] (cf. Guckenheimer and Holmes [12]). Simulation of this and the following higher-dimensional systems allows us to check the validity of our assumption that only the most unstable eigenvalue and the r.m.s. noise level affect the passage time distribution at leading order (cf. § 2).

Before presenting the results it is necessary to recall an important feature of the heteroclinic orbit structure of (4.1). Armbruster, Guckenheimer, and Holmes [2] show that for $\varepsilon = 0$ and a fairly wide range of μ_j , e_{ij} , (4.1) has attracting heteroclinic cycles. Each such cycle involves connections between two diametrically opposite points $z_2 = \sqrt{-\mu_2/e_{22}} e^{i\phi}$, $\sqrt{-\mu_2/e_{22}} e^{i\phi+\pi}$ on the circle of pure two-mode equilibria $z_1 = 0$, $|z_2| = \sqrt{-\mu_2/e_{22}}$. Since the cycle involves two saddle points, the local estimate (2.27)–(2.28) must be counted twice, leading to a modification of our general result (2.32):

$$(4.2) \quad T_{O(2)} = K_0 + \frac{2}{\lambda_u} (|\ln(\varepsilon)| + K_1).$$

The eigenvalues at the fixed points in question are given by the formulae

$$(4.3) \quad \begin{aligned} \lambda_u &= \mu_1 - \frac{\mu_2 e_{12}}{e_{22}} + \sqrt{-\frac{\mu_2}{e_{22}}} \quad (>0), \\ -\lambda_{s_1} &= \mu_1 - \frac{\mu_2 e_{12}}{e_{22}} - \sqrt{-\frac{\mu_2}{e_{22}}} \quad (<0), \\ -\lambda_{s_2} &= -2\mu_2 \quad (<0). \end{aligned}$$

The fourth eigenvalue is zero and its eigenvector is tangent to the circle of equilibria, which correspond to orbits of the symmetry group. As Armbruster, Guckenheimer, and Holmes [2] show, this and the magnitude of the second stable eigenvalue λ_{s_2} are irrelevant to the stability analysis of the cycles and thus λ_{s_1} plays the role of λ_s in § 2. Attractivity is guaranteed if $\lambda_u - \lambda_{s_1} < 0$ or $\mu_1 - \mu_2 e_{12}/e_{22} < 0$ and $\mu_2 > 0$ [2, Thm. 5.5]. The parameter values selected for the simulations that follow satisfy these inequalities.

Figure 5 shows mean passage times versus r.m.s. noise level ε for three different choices of parameter values, giving a variation in unstable eigenvalue λ_u of 0.196 to 0.226. In the fitted expression the constant K_0 is roughly the time to travel the two loops of the complete cycle. K_1 is estimated to give a good fit to the data for the chosen K_0 . As expected, K_0 is nearly the same for each curve, since the variation of the vector field from one case to the other is slight.

In this case we did not attempt to estimate global loop passage times separately, or to explicitly divide our simulations into global and local portions, as in § 3. (It is easy to do this, as in the Duffing case, by appealing to the integrable limit of (4.1) in which the μ_{ij} (and hence $|z_j|$) are taken very small and can be neglected in the limit $\mu_j \rightarrow \infty$.) However, we note that, in the r.m.s. noise level range studied in our simulations, the leading order form (4.2) for the mean passage time fits the data extremely well.

The final set of simulations were performed on a ten-dimensional $O(2)$ symmetric system that describes the interaction among five complex spanwise Fourier modes in a turbulent boundary layer. The model is derived and described in Aubry et al. [5] where details of the equations and specific coefficient values may be found. This system

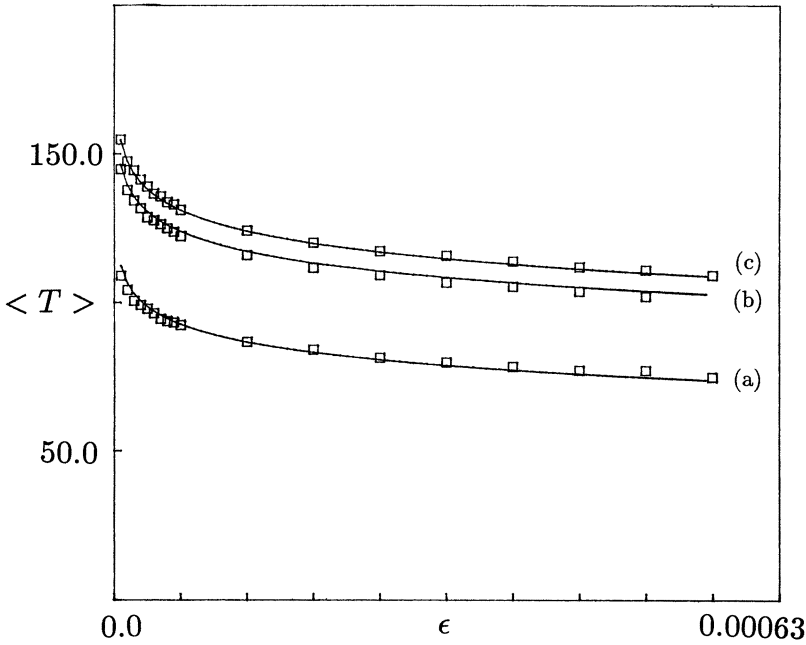


FIG. 5. Simulations of the $O(2)$ invariant two-mode system (4.1) $e_{11} = -4$, $e_{12} = -1$, $e_{21} = -2$, $e_{22} = -2$. (a) $\mu_1 = 0.05$, $\mu_2 = 0.2$, $\lambda_u = 0.266$; (b) $\mu_1 = -0.01$, $\mu_2 = 0.2$, $\lambda_u = 0.206$; (c) $\mu_1 = -0.02$, $\mu_2 = 0.2$, $\lambda_u = 0.196$; Sample size = 500 trials. (See Armbruster, Guckenheimer, and Holmes [2] for details.)

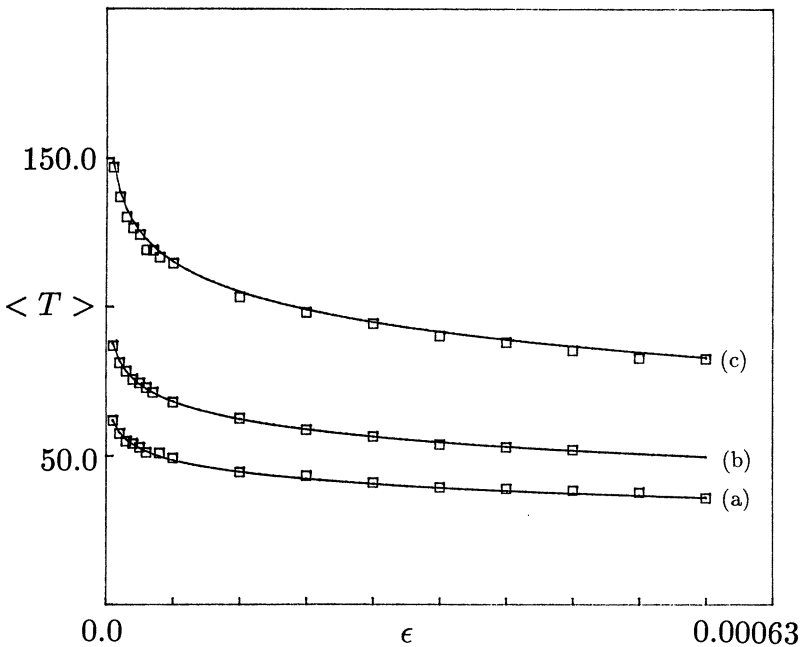


FIG. 6. Simulations of the $O(2)$ invariant five-mode boundary layer model. (a) $\alpha = 1.45$, $\lambda_u = 0.3434$; (b) $\alpha = 1.5$, $\lambda_u = 0.2375$; (c) $\alpha = 1.55$, $\lambda_u = 0.1362$; sample size = 200 trials. (See Aubry et al. [5] for details.)

is known to possess attracting heteroclinic cycles over a range $1.35 < \alpha < 1.61$ in the “free” parameter α , which governs energy loss to higher wavenumber modes ignored in the low-order truncation. The principal effect of varying α is to vary the real part of a pair of complex conjugate unstable eigenvalues at the circle of saddle points involved in the heteroclinic cycles. Since the structure is basically the same as in the two-mode model (4.1), the asymptotic formula (4.2) is again applicable.

Figure 6 shows the results of simulations for three values of α , with λ_u varying between 0.3434 and 0.1362. Again we plot mean passage time versus r.m.s. noise amplitude and again the comparison with equation (4.2) is excellent. Here the coefficients K_0 , K_1 were determined from a single data set ($\alpha = 1.5$). Reference [5] contains pictures of typical time series for this system.

We conclude that the theory of § 2 provides a good description of the effects of additive random noise of multidimensional systems possessing attracting heteroclinic cycles.

5. Conclusions and implications. We conclude this paper with a brief discussion of the implications of our analysis for the modeling of practical problems. In the boundary layer model studies of Aubry et al. [5], the small additive noise term arises naturally in the following way. The Navier–Stokes equations are considered in the wall region of a turbulent boundary layer. Periodic boundary conditions are taken in the spanwise and streamwise direction and velocities vanish on the wall itself, but the boundary condition at the outer edge of the layer approximates a free surface. Since velocities here are nonzero, in the Galerkin projection process a boundary pressure term survives after integration by parts. Physically, this corresponds to coupling between the inner wall layer and the outer part of the boundary layer. Aubry et al. [5] estimate the pressure term from numerical computations of Moin [15]. It is certainly not white noise and the various components in the projected ordinary differential equations are not uncorrelated, but the pressure term does act as a small random perturbation preventing close approaches to the saddle point in the attracting heteroclinic cycles. (The perturbation is two to three orders of magnitude smaller than the typical deterministic terms.) In this way the durations between heteroclinic “events” tend to equilibrate much as in the theory developed in this paper. In fact, the asymptotic form (4.2) (cf. (2.32)) fits the simulations reported by Aubry et al. [5] reasonably well, although not as well as the white noise results of § 4 (Fig. 6), which also may be due to a limited number of trials in the earlier case.

In the boundary layer application the heteroclinic orbits are thought to correspond to turbulent “bursting” or sweep and ejection events: the solution remains quiescent near a saddle point for a period and then relatively rapidly transits to another saddle point, which is an image of the first under a symmetry group element. In this process a quasi-steady velocity field in the fluid is violently perturbed and then reforms. The quiescent fields are associated with coherent structures in the turbulent flow field. In the absence of the pressure perturbation, the duration between events increases without bound, since the heteroclinic cycle is attracting. The small pressure signal therefore acts as a trigger that promotes heteroclinic transits without changing their general form. The pressure term causes a random distribution of quiescent periods with a clearly defined mean, which is well estimated by our theory. In this application, ε , the noise (pressure) level, can be thought of as a variable characteristic of the outer boundary layer, whereas λ_u , the unstable eigenvalue, is a characteristic of the inner layer. Thus our theory predicts that the mean duration between burst events should scale with a combination of the inner and outer variables. This has important

implications in the understanding and modification of turbulent boundary layers (e.g., Alfredsson and Johansson [1]).

As Armbruster, Guckenheimer, and Holmes [2], [3] explain, $O(2)$ symmetric heteroclinic cycles are likely to play an important role in determining the dynamics of many translation and reflection invariant PDEs. We therefore feel that the general features of the boundary layer application outlined above will recur in other applications. These general features of the process can be summarized thus: in the unperturbed case a topologically simple attracting set, a homoclinic loop or heteroclinic cycle, exists. All orbits starting sufficiently close to this set approach this set and spend increasing periods near the saddle points within it as $t \rightarrow \infty$. The addition of weak additive noise does not change the structure of solutions in the phase space much, but it causes a radical change in and leads to a selection of *timescales*. Our theory permits us to predict the probability distribution of passage times from information on the system linearized at a saddle point, and to provide a simple characterization of mean passage times, which depend only on the strongest unstable eigenvalue λ_u and the r.m.s. noise level at leading order. The random perturbation is generating a typical timescale. A similar phenomenon of timescale generation in a two-dimensional system near a saddle node bifurcation has been studied by Sigeiti and Horsthemke [18].

Acknowledgments. The authors thank the referees for pointing out many small errors and the fact that assumption (A3) is necessary unless a more complex analysis of the vector Kolmogorov equation is undertaken.

REFERENCES

- [1] P. H. ALFREDSSON AND A. V. JOHANSSON, *On the determination of turbulence generating events*, J. Fluid Mech., 139 (1984), pp. 325–342.
- [2] D. ARMBRUSTER, J. GUCKENHEIMER, AND P. HOLMES, *Heteroclinic cycles and modulated travelling waves in systems with $O(2)$ symmetry*, Phys. D., 29 (1988), pp. 257–282.
- [3] ———, *Kuramoto–Sivashinsky dynamics on the center unstable manifold*, SIAM J. Appl. Math., 49 (1989), pp. 676–691.
- [4] L. ARNOLD, *Stochastic Differential Equations*, John Wiley, New York, 1974.
- [5] N. AUBRY, P. HOLMES, J. LUMLEY, AND E. STONE, *The dynamics of coherent structures in the wall region of a turbulence boundary layer*, J. Fluid Mech., 192 (1988), pp. 115–173.
- [6] L. BREIMAN, *Probability*, Addison-Wesley, Reading, MA, 1968.
- [7] F. M. BUSSE, *Transition to turbulence in Rayleigh–Bénard convection*, in Hydrodynamic Instabilities and the Transition to Turbulence, H. L. Swinney and J. P. Gollub, eds., Springer-Verlag, Berlin, New York, 1981, pp. 97–137.
- [8] F. M. BUSSE AND K. E. HEIKES, *Convection in a rotating layer: a simple case of turbulence*, Science, 208 (1980), pp. 173–175.
- [9] D. R. J. CHILLINGWORTH, *Differential Topology with a View to Applications*, Pitman, London, 1976.
- [10] D. FARMER, *Deterministic noise amplifiers*, Los Alamos Report LA-UR-84-3628, Los Alamos National Laboratories, Los Alamos, NM, 1984.
- [11] J. GUCKENHEIMER AND P. HOLMES, *Nonlinear Oscillations, Dynamical Systems and Bifurcations of Vector Fields*, Springer-Verlag, Berlin, New York, 1983; corrected second printing, 1986.
- [12] ———, *Structurally stable heteroclinic cycles*, Math. Proc. Cambridge, Philos. Soc., 103 (1988), pp. 189–192.
- [13] C. JONES AND M. R. PROCTOR, *Strong spatial resonances and travelling waves in Bénard convection*, Phys. Lett. A, 121 (1987), pp. 224–227.
- [14] Y. KIFER, *The exit problem for small random perturbations of dynamical systems with a hyperbolic fixed point*, Israel J. Math., 40 (1981), pp. 74–96.
- [15] P. MOIN, *Probing turbulence via large eddy simulation*, in Proc. AIAA 22nd Aerospace Sciences Meeting, Reno, NV, January 9–12, 1984.
- [16] Y. POMEAU AND P. MANNEVILLE, *Intermittent transition to turbulence in dissipative dynamical systems*, Commun. Math. Phys., 74 (1980), pp. 189–197.

- [17] M. K. PROCTOR AND C. JONES, *The interaction of two spatially resonant patterns in thermal convection 1: exact 1:2 resonance*, J. Fluid Mech., 188 (1988), pp. 301–335.
- [18] D. SIGETI AND W. HORSTHEMKE, *Pseudo regular oscillations induced by external noise*, J. Statistic Phys., 54 (1989), pp. 1217–1222.
- [19] L. P. SILNIKOV, *A case of the existence of a denumerable set of periodic motions*, Soviet Math. Dokl., 6 (1965), pp. 163–166.
- [20] ———, *The existence of a denumerable set of periodic motions in four dimensional space in an extended neighborhood of a saddle-focus*, Soviet Math. Dokl., (1967), pp. 54–58.
- [21] S. SMALE, *Differentiable dynamical systems*, Bull. Amer. Math. Soc., 73 (1967), pp. 747–817.
- [22] S. WIGGINS, *Global Bifurcations and Chaos-Analytical Methods*, Springer-Verlag, Berlin, New York, 1988.